isoforms, including MITF-A, MITF-B, MITF-C, MITF-H, and MITF-M, and MITF-M is the melanocyte-specific type (Tachibana, 1997; Udono *et al.*, 2000; Shibahara *et al.*, 2001). MITF regulates the expression of melanocyte differentiation markers, including tyrosinase, tyrosinase-related protein, and dopachrome tautomerase (DCT), all of which are required for pigmentation (Carreira *et al.*, 2000). MITF is one of the genes involved in tumor growth and the metastasis of melanoma (Vachtenheim *et al.*, 2001, Nyormoi and Bar-Eli, 2003). However, transcriptional target genes of MITF that regulate melanoma tumorigenicity or metastasis have not yet been elucidated. Moreover, since MITF alone has low or no oncogenic activity, a cofactor(s) that cooperatively functions with MITF may be necessary for the transformation of melanocytes.

In this study, we first demonstrated that STAT3 and MITF cooperatively induce cellular transformation *in vitro*. We also identified c-*fos* as a target gene of STAT3 and MITF using microarray analysis. The induction of the c-*fos* gene is necessary for the anchorage-independent growth of NIH-3T3 cells transformed with STAT3C and MITF. Our study provides a novel role of STAT3 in melanocyte proliferation and tumor growth of melanoma.

Results

Screening for STAT3C cofactors for cellular transformation

We and others have shown that NIH-3T3 cells expressing STAT3C or wild-type STAT3, which is activated by the type C hepatitis virus (HCV) core protein, possess a colony-forming potential in soft-agar and tumorigenicity in nude mice (Yoshida *et al.*, 2002). However, the number and size of the colonies and tumor size by the expression of active STAT3 are much smaller than those of NIH-3T3 cells transformed with v-src (Bromberg *et al.*, 1999; Yoshida *et al.*, 2002). Therefore, the constitutive activation of STAT3 may not be sufficient for full transformation. With this in mind, we screened cofactors that induce full transformation in cooperation with activated STAT3 by using retrovirus cDNA transfer (Kitamura *et al.*, 1995). NIH-3T3 cells expressing STAT3C (STAT3C-3T3) were infected with the HeLa cell retroviral cDNA library (2×10^6 independent clones) and plated into soft-agar medium. After 3 weeks of incubation, two large colonies were formed and the integrated cDNAs were recovered by PCR and sequenced. One colony contained MITF cDNA with N-terminal 104 amino acids deletion compared with MITF-M (ΔN-MITF), and the other colony included full-length granulin cDNA that has been shown to induce colony formation in soft-agar in NIH-3T3 cells (Zanocco-Marani *et al.*, 1999). The ATG of the exon 3 of the MITF gene was utilized as the first AUG codon in ΔN-MITF (Figure 1a). N-terminal truncation resulted in a missing N-terminal glutamine-rich region, but ΔN-MITF retained DNA-binding and transactivation domains.

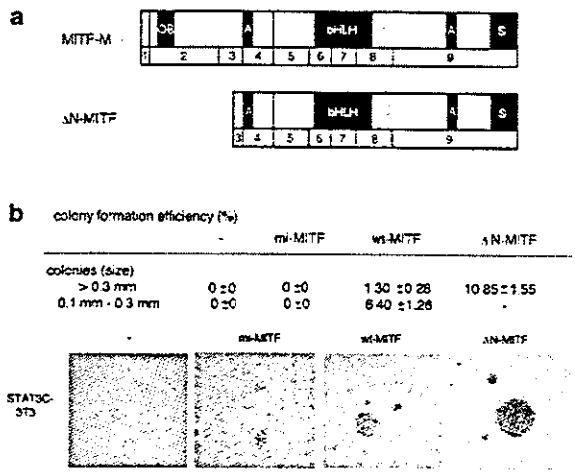

Figure 1 Transforming potential with a combination of MITF and STAT3C. (**a**) Structures of MITF-M and our screening clone, ΔN-MITF. The numbers shown under MITF isoforms indicate exons. The glutamine-rich basic region (QB), the transcriptional activation domain (A), the bHLH-LZ structure, and the serine-rich domain (S) are indicated. (**b**) STAT3C-transformed 3T3 (STAT3C-3T3) cells were infected with the pMX empty vector, pMX-mi-MITF, wt-MITF, or ΔN-MITF and plated into soft-agar medium. On day 21, colonies were counted and photographed

MITF-induced anchorage-independent growth in cooperation with STAT3C

The inserted cDNAs subcloned into the retroviral vector, pMX-IRES-EGFP, were introduced into parental NIH-3T3 cells or STAT3C-3T3 cells and then plated into soft-agar medium. N-terminal-truncated MITF induced the cellular transformation of STAT3C-3T3, but not parental NIH-3T3 cells, whereas granulin cDNA induced anchorage-independent cell growth in both NIH-3T3 cells and STAT3C-3T3 cells (Figure 1b and data not shown). Therefore, ΔN-MITF has the potential to induce the anchorage-independent growth of NIH-3T3 cells in cooperation with STAT3C. We also found that full-length (wt-) MITF could lead to anchorage-independent growth of NIH-3T3 cells in cooperation with STAT3C (Figure 1b). However, ΔN-MITF showed greater colony-forming activity, both in size and number, than wt-MITF.

We then compared the cellular morphology of transfectants. It has been reported that the forced expression of MITF in NIH-3T3 cells results in refractile cell morphology, which resembled dendritic cells and melanocytes (Tachibana, 1997). We also observed that ΔN-MITF-infected NIH-3T3 cells showed dendritic cell-like morphological changes (Figure 2a). However, as shown in Figure 2b, STAT3C-3T3 cells expressing wt-MITF or ΔN-MITF displayed some of the morphological changes associated with fibroblast transformation, that is, elongated shape and rounding.

Constitutive activation of STAT3 in melanoma cells

We then examined STAT3 activation in melanoma cells in which MITF plays an important role in transformed

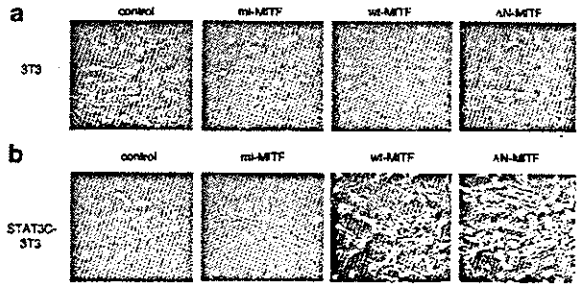

Figure 2 Cytology of MITF-infected 3T3 and STAT3C-3T3 cells. 3T3 and STAT3C-3T3 were infected with the pMX empty vector, pMX-mi-MITF, wt-MITF, or ΔN-MITF. wt-MITF and ΔN-MITF induced morphological change in both 3T3 (a) and STAT3C-3T3 (b)

phenotypes. As shown in Figure 3a, some melanoma cell lines, B16F10, G361, MMAc, and HMV-II, showed constitutive phosphorylation of STAT3. We examined whether MITF induced the constitutive activation of STAT3. Immunoblotting with an anti-phosphorylated STAT3-specific antibody revealed that phosphorylation occurred in tyrosine 705 (Y705) of STAT3 in STAT3C-3T3 cells (Figure 3b). wt-MITF and ΔN-MITF did not affect phosphorylation states of STAT3 in NIH-3T3 cells (Figure 3b). As shown in Figure 3c, MITF had little effect on or rather suppressed STAT3-dependent APRE-luciferase activity. These data indicate that STAT3 is often constitutively activated in melanoma cells, but the mechanism is probably independent of MITF expression. Furthermore, MITF-transactivation activity was not affected by STAT3C (data not shown). Therefore, we speculated that an oncogenic target gene(s) could be induced by the cooperative action of STAT3 and MITF.

Microarray screening for target genes of STAT3C and MITF

To identify target genes of MITF and STAT3, a microarray-based screen was undertaken. Total RNA was isolated from ΔN-MITF-infected NIH-3T3 (ΔN-MITF-3T3), STAT3C-3T3, and ΔN-MITF-infected STAT3C-3T3 (ΔN-MITF/STAT3C-3T3) cells and subjected to Affymetrix microarray analysis (about 12000 genes). As summarized in Figure 4a, seven genes in ΔN-MITF/STAT3C-3T3 cells were identified as more than 10-fold upregulated genes compared with ΔN-MITF-3T3 and STAT3C-3T3 cells. Most of the genes were mast cell or melanocyte-specific genes and chemokines, and the upregulation of these genes was confirmed by RT–PCR analysis (Figure 4b). Among these seven genes, the upregulation of c-*fos* is particularly interesting because c-*fos* is a component of the AP-1 transcription factor and known to be an oncogene. The functions of AP-1, composed of Fos family proteins (c-Fos, Fra-1, Fra-2, and FosB) and Jun family proteins (c-Jun, JunB, and JunD), were shown to play important roles not only in normal cell growth but also in several transformed cells induced by oncogenes (Ui *et al*., 2000). Therefore,

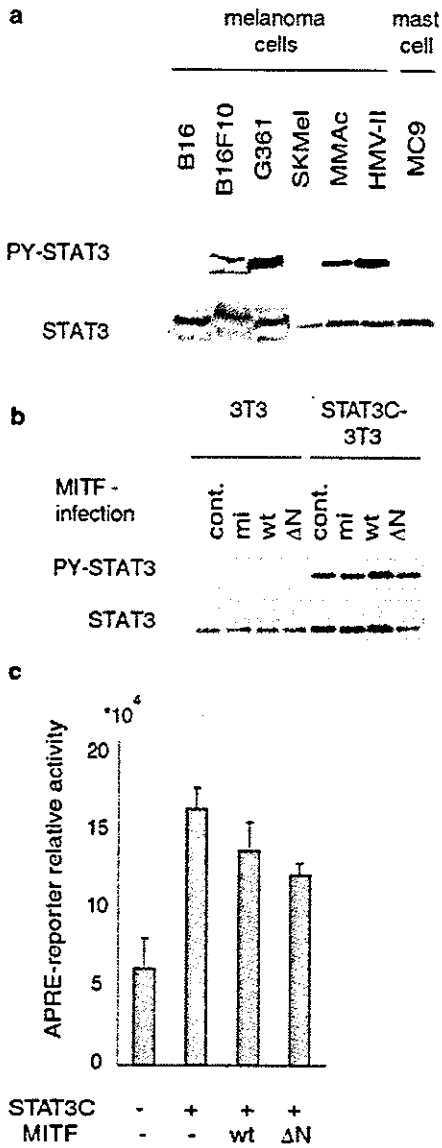

Figure 3 MITF and STAT3C do not directly activate each other. (a and b) Phosphorylation of STAT3 was detected by Western blotting with anti-phosphorylated Tyr705 of the STAT3-specific antibody. Lysate from cell lines of melanoma cells and mast cells (a) or 3T3 and STAT3C-3T3 cells infected with the pMX empty vector, pMX-mi-MITF, wt-MITF, or ΔN-MITF (b) were examined. (c) HEK293 cells were transfected with a plasmid mixture containing the APRE-luciferase reporter gene (0.04 μg) and the β-galactosidase gene (0.1 μg). To examine the MITF-dependent APRE-luciferase activity, cDNA of STAT3C (0.2 μg) and MITF (0.1 μg) was also introduced. Data normalized with the β-galactosidase activity from triplicate experiments are shown

we confirmed the upregulation of the c-*fos* gene by Northern blotting. As shown in Figure 4c, c-*fos* was consecutively expressed in ΔN-MITF/STAT3C-3T3 cells, but was not detected in quiescent 3T3 cells. We also detected the endogenously high expression of c-*fos*

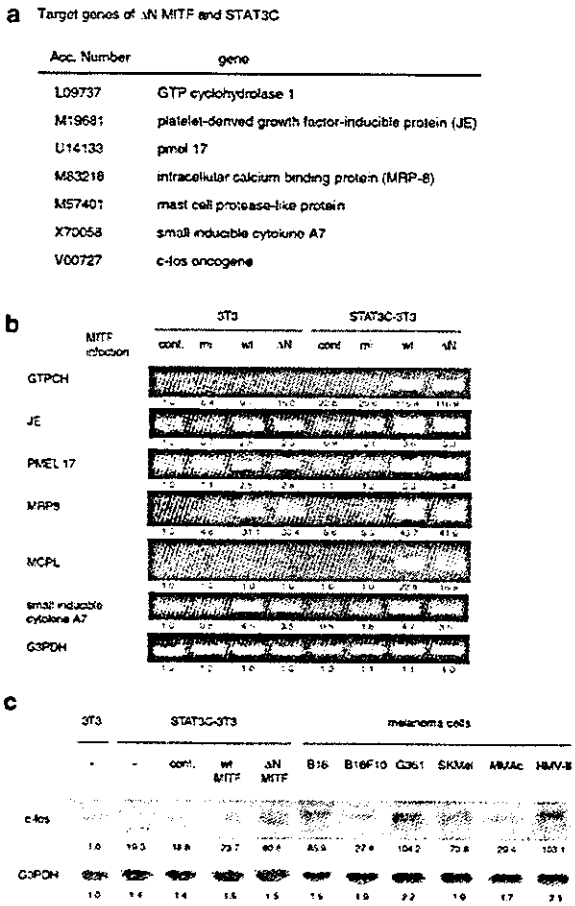

Figure 4 Expression of genes upregulated by MITF and STAT3C. (**a**) In microarray analysis, seven genes in 3T3 cells expressing both ΔN-MITF and STAT3C were found as >10-fold upregulated genes compared with STAT3C-3T3 or ΔN-MITF single transfectants. (**b**) Upregulation in six of the genes detected by microarray analysis. The mRNA expression level was evaluated by the RT–PCR method in 3T3 or STAT3C-3T3 cells infected with the pMX empty vector, pMX-mi-MITF, wt-MITF, or ΔN-MITF. The intensity of the PCR band was quantified with NIH image software. (**c**) Northern blotting analysis of the c-*fos* oncogene. 3T3 cells, STAT3C-3T3 cells uninfected or infected with empty vector, wt-, or ΔN-MITF viruses, and six kinds of melanoma cell lines were examined with RNA probes of c-*fos* and G3PDH

in several melanoma cell lines (Figure 4c), suggesting that the constitutive expression of c-*fos* contributes to the oncogenesis of melanoma.

STAT3 and MITF directly bind to the promoter region of c-fos

It has been shown that the c-*fos* proximal promoter region contains a single STAT3-binding site in the SIE region (Shibuya *et al*., 1994). We also noticed many MITF-binding motifs (CANNTG; E-box) (Tsujimura *et al*., 1996) in the promoter region (Figure 5a). To confirm that c-*fos* activation was cooperatively induced by MITF and STAT3C, a reporter gene assay using c-*fos* promoter luciferase constructs (Hatakeyama *et al*., 1992) was carried out. The transcriptional activity of c-*fos* was significantly increased by the transient expression of wt- or ΔN-MITF and STAT3C in HEK293 cells. MITF-induced c-*fos* promoter activation was further stimulated by leukemia inhibitory factor (LIF), which activates endogenous STAT3 (Figure 5b and data not shown).

Next, we examined the region of the c-*fos* promoter responsible for the interaction of MITF and STAT3. The c-*fos* promoter construct contains five potential MITF-binding sites. Using mutated or truncated forms of the c-*fos* promoter, we found that the SIE region is important for activation by STAT3 and an MITF-binding motif in the SRE region is essential for promoter activation by MITF (Figure 5c).

To confirm the direct binding of STAT3 and MITF to the c-*fos* promoter region, DNA-binding assay (Figure 5d) as well as chromatin immunoprecipitation (ChIP) assay (Figure 5e) were performed. First, nuclear extracts from 293T cells transfected with Myc-tagged ΔN-MITF and STAT3C or from cells stimulated with or without LIF were incubated with beads conjugated with oligonucleotides of the human c-*fos* promoter sequence, including the SIE and the SRE (55 mer). As shown in Figure 5d, MITF (lanes 2, 4, and 6) as well as both phosphorylated endogenous STAT3 (lanes 3 and 4) and STAT3C (lanes 5 and 6) bound to the oligonucleotides of the c-*fos* promoter region *in vitro*. Non-phosphorylated STAT3 without LIF stimulation (lanes 1 and 2) did not bind to the oligonucleotide beads, suggesting a specific interaction of activated STAT3 and the DNA.

For ChIP assay (Figure 5e), the crosslinked chromatins from wt-MITF/STAT3C-3T3 cells and ΔN-MITF/STAT3C-3T3 cells as well as melanomas (G361 and HMV-II) in which STAT3 was consecutively phosphorylated were immunoprecipitated with STAT3- or MITF-specific antibodies. The crosslinked protein was then removed from DNA by proteolysis. Finally, the immunoprecipitated DNA was analysed by PCR to detect the c-*fos* promoter region. As shown in Figure 5e, the anti-STAT3 antibody and the anti-MITF antibody precipitated the c-*fos* promoter SIE region and the MITF-binding motif in the SRE region, respectively.

Dominant-negative mutant of AP-1 inhibited cellular transformation of MITF/STAT3C-3T3

To investigate the contribution of the c-*fos* gene in the anchorage-independent growth of MITF/STAT3C-3T3 cells, we introduced a dominant-negative mutant of AP-1 into these cells. We used a retrovirus carrying SupJunD-1, which has an N-terminal deletion of the transactivation domain of c-Jun. We have shown that the SupJunD-1 virus suppresses the transactivation activity of AP-1 and inhibits colony formation in soft agar of various types of tumor cells (Ui *et al*., 2000). As shown in Figure 6, the dominant-negative AP-1

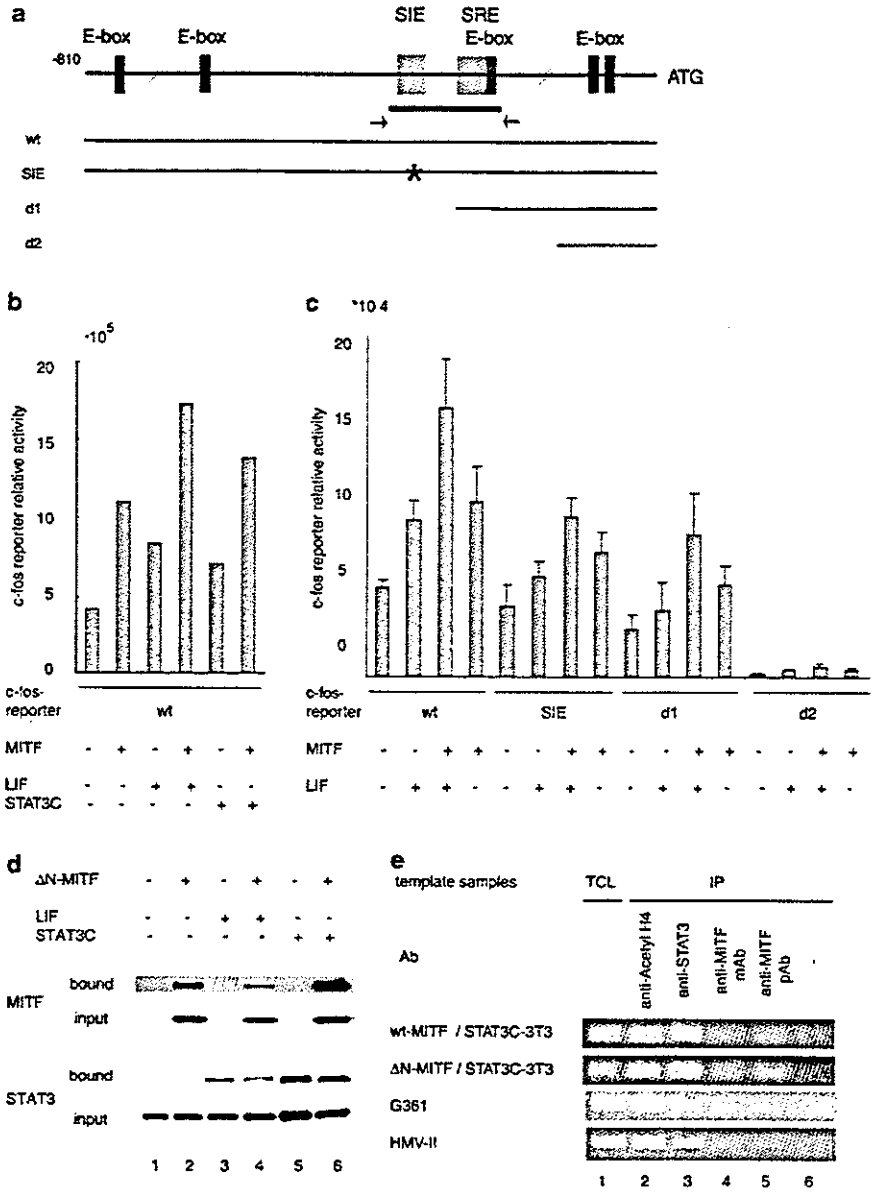

Figure 5 MITF and STAT3C directly binds to the promoter region of c-fos. (**a**) A diagram of the c-*fos*-luciferase reporter gene containing five E-boxes, potential MITF-binding motifs, and the SIE region known as a binding site of STAT3. Asterisks indicate mutations in SIE, and two deletion mutants (d1 and d2) are shown. The bold bar shows the region used for the DNA-binding assay and arrows show the PCR primers for ChIP assay. (**b** and **c**) *Reporter assay*. HEK293 cells were transfected with a plasmid mixture containing the c-*fos*-luciferase reporter gene (2 ng), the β-galactosidase gene (0.1 μg), STAT3C (0.2 μg), and the wt-MITF plasmid (**b**, 200 ng, and **c**, 10 ng). After transfection, cells were incubated in the presence or absence of 10 ng/ml LIF for 8 h, and cell extracts were prepared. Data normalized with the β-galactosidase activity from triplicate experiments are shown. (**d**) *DNA-binding assay*. 293T cells were transfected with the pcDNA3-Myc-ΔN-MITF and pRcCMV-STAT3C and stimulated with 10 ng/ml LIF for 6 h, and the nuclear extracts were prepared. The DNA-binding proteins bound to the oligonucleotide-conjugated beads were analysed by immunoblotting with anti-STAT3 and anti-Myc antibodies. (**e**) ChIP assay was performed to determine the binding of MITF and STAT3 to the promoter region of c-*fos*. wt- or ΔN-MITF-infected STAT3C-3T3 was determined *in vitro*, and the melanoma cells G361 and HMV-II were examined *in vivo*. Chromatin complexes were immunoprecipitated with anti-acetylated histone H4, anti-STAT3, and monoclonal or polyclonal anti-MITF antibodies

significantly suppressed the anchorage-independent growth of wt- or ΔN-MITF-infected STAT3C-3T3 cells. These data support our notion that c-*fos* induction is one of the mechanisms of increased anchorage-independent growth of MITF/STAT3C-expressing cells.

colony formation efficiency (%)

	retrovirus infection	wt-MITF	ΔN-MITF
colonies (size)			
> 0.3 mm	-	1.30 ± 0.28	10.85 ± 1.55
	cont.	1.11 ± 0.41	6.83 ± 3.31
	dnAP-1	0.03 ± 0.05	1.33 ± 0.90
0.1 mm - 0.3 mm	-	6.40 ± 1.26	-
	cont.	4.98 ± 1.88	-
	dnAP-1	0.84 ± 0.88	-

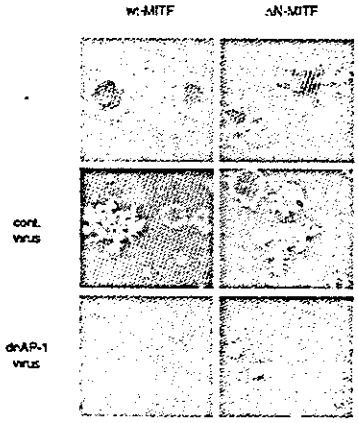

Figure 6 Expression of dominant-negative AP-1 inhibits anchorage-independent growth of MITF/STAT3C-expressing cells. wt- or ΔN-MITF-infected STAT3C-3T3 cells were infected with retrovirus carrying dominant-negative AP-1 (dnAP-1) or an empty vector by the retrovirus at moi = 10. Cells were selected with puromycin and then plated into soft-agar medium. On day 21, colonies were counted and photographed. Data from triplicate experiments are shown

Discussion

In this study, we identified MITF as a collaborative factor of STAT3 for cellular transformation. Many factors have been shown to interact with and activate (or in some cases inactivate) STAT3. For example, we have shown that the HCV core protein directly interacts with STAT3 and induces phosphorylation and activation (Yoshida *et al*., 2002). Nakayama *et al*. (2002) reported that a nuclear zinc-finger protein EZI enhances the nuclear retention and transactivation of STAT3. PIAS3 (Levy *et al*., 2002), cyclinD (Matsui *et al*., 2002), and GRIM-19 (Lufei *et al*., 2003) also interact directly with STAT3, but inhibit transcriptional activity. Most of these factors are isolated as a physical binding protein with STAT3. In this study, by using functional expression screening, we showed that STAT3 and MITF interact functionally, but not physically. A common target of STAT3 and MITF is found to be c-*fos*, which may participate in transformation by constitutively active STAT3 and MITF. Our functional cloning strategy using retroviral cDNA transfer will provide an additional candidate for the cofactor that modulates the function of STAT3. Furthermore, in this study we demonstrated that the microarray technique is a powerful tool to identify a target gene that is cooperatively induced by two distinct classes of transcription factors.

MITF consists of at least five isoforms, MITF-A, MITF-B, MITF-C, MITF-H, and MITF-M, differing at their N-termini and expression patterns (Tachibana, 1997; Udono *et al*., 2000; Shibahara *et al*., 2001). However, the clone (ΔN-MITF) we obtained from the HeLa cell library has an N-terminal deletion, which is shorter than other reported forms. Since mRNA corresponding to ΔN-MITF has not been reported, we speculate that ΔN-MITF is a product of the incomplete elongation of cDNA by reverse transcriptase. Nevertheless, ΔN-MITF seems to be a more potent inducer for a transformed phenotype of NIH-3T3 cells (Figure 1) and c-*fos* induction (Figure 4). In addition to the previously characterized acidic activation domain necessary for melanocyte differentiation, a second potential activation domain is shown to be located between amino acids 140 and 185 (Mansky *et al*., 2002), and ΔN-MITF contains these regions. Therefore, the N-terminal, with about 100 amino acids of MITF-M, may be a negative regulatory domain. This region contains a glutamine-rich basic region (QB), but the function of this region has not been elucidated. Most notably, Ser 73 of MITF-M is a predicted MAP kinase-phosphorylation site and is implicated in p300/CBP recruitment (Hemesath *et al*., 1998) and reduced MITF protein stability (Kim *et al*., 2003). Since ΔN-MITF lacks this Ser 73, dN-MITF may be more stable than wt-MITF.

Several types of functional interactions between STAT3 and MITF have been proposed. The protein inhibitor of activated STAT3 (PIAS3) has been shown to bind to a b-HLH-Zip domain of MITF, resulting in the suppression of MITF-induced transcriptional activity (Levy *et al*., 2002). However, it has been reported that STAT3 does not interfere, either *in vitro* or *in vivo*, with the interaction between PIAS3 and MITF. This finding is consistent with our data showing that STAT3 does not affect MITF transcriptional activity (data not shown) and MITF does not interfere with STAT3 transcriptional activity (Figure 3c). Recently, Kamaraju *et al*. (2002) reported that IL-6 receptor/IL-6 chimera induces a loss of melanogenesis preceded by a sharp decrease in MITF mRNA and gene promoter activity in B16/F10.9 melanoma cells. IL6RIL6 stimulates gp130, leading to the rapid activation of STAT3, which downregulates Pax3, a paired homeodomain factor regulating MITF mRNA levels and the development of melanocytes. Therefore, in this case, MITF downregulation by STAT3 is indirect, and the mechanism of Pax3 downregulation by STAT3 is not clear. The Pax3 downregulation in IL6RIL6-induced F10.9 cells leads to growth arrest and transdifferentiation to a glial cell phenotype. Therefore, the genetic interaction between MITF and STAT3 seems to be complicated and probably different among cell types.

We found that the c-*fos* gene is a common target of STAT3 and MITF, which probably contributes to transformation. Microarray analysis also revealed that

the c-*fos* gene is strongly upregulated by MITF in primary melanocytes (McGill *et al.*, 2002). In agreement with this notion, STAT3 was frequently phosphorylated in several human melanoma cell lines (Figure 3a). However, while B16 and SKMel cells are negative for STAT3 phosphorylation, the same cells do express c-*fos*. Apparently, STAT3-independent mechanism of c-*fos* induction is present in these melanoma cells. Finding such mechanisms of c-*fos* expression in these cells may provide a new clue for understanding the role of c-*fos* for the generation of melanomas.

Promoter analysis and ChIP assay indicated that STAT3 and MITF can bind to the c-*fos* promoter and activate this promoter independently. Reporter gene analysis suggested that the effect of MITF and STAT3 on the c-*fos* promoter are additive rather than cooperative (Figure 5b). This is consistent with our observation that there is no direct physical interaction between MITF and STAT3. Nevertheless, high levels of c-*fos* expression and transformation of NIH-3T3 cells are dependent on both STAT3 and MITF. In addition to promoter activation, another mechanism of c-*fos* expression, such as stabilization of c-*fos* mRNA, may present in the cooperative effect of STAT3 and MITF. Furthermore, a previous report demonstrated that wt- and mi-MITF bind to the c-Fos protein. In particular, mi-MITF prevents c-Fos from being transported to the nucleus, and this may be a reason for the osteopetrosis of mi/mi mutant mice (Sato *et al.*, 1999). wt-MITF was also shown to bind to c-Jun and enhance the transactivation of the MMCP-7 gene, while complexes of mi-MITF and c-Jun were predominantly found in the cytoplasm and suppressed transactivation (Ogihara *et al.*, 2001). Thus, MITF could be involved in AP-1 activation not only by inducing c-*fos* but also by interacting with AP-1 itself. The fact that a dominant-negative AP-1 (SupJunD) suppressed colony formation of transformants expressing both MITF and STAT3C suggests that AP-1 can be a therapeutic target of melanoma.

In addition to c-*fos*, we found several interesting genes that are cooperatively induced by STAT3 and MITF (Figure 4a). GTP cyclohydrase-1 and mast cell proteases are probably involved in melanocyte and mast cell functions. PMEL17 is also known as an MITF-inducible pigment cell-specific gene and a melanosomal matrix protein, which may function as a structural protein in melanogenesis (Kobayashi *et al.*, 1994). JE and A7 are chemokines that are induced by immunoglobulin (Ig) E plus antigen stimulation in mast cells. (Burd *et al.*, 1989; Kulmburg *et al.*, 1992; Ong *et al.*, 1993). Therefore, STAT3/MITF target genes are strongly linked to the function of mast cells and melanocytes, which constitutively express MITF. This finding implies that STAT3 (or other STATs) may be involved in mast cell and melanocyte functions by inducing genes in cooperation with MITF. It is interesting that IL3, which activates STAT5, is a mast cell growth factor *in vitro*. The functions of STATs in mast cells and melanocytes are under investigation.

Materials and methods

Cell culture and transfection

NIH3T3 and HEK293 cells were cultured in Dulbecco's modified Eagle's medium supplemented with 10% CS. STAT3C-transformed 3T3 (STAT3C-3T3) cells (Yoshida *et al.*, 2002) were cultured in DMEM supplemented with 10% CS containing 0.8 mg/ml G418. PLAT-E, a packaging cell line (Morita *et al.*, 2000) was maintained in DMEM with 10% FCS containing blasticidin S (10 mg/ml) and puromycin (1 mg/ml). Melanoma cell lines were cultured in the following medium containing 10% FCS, B16 and B16F10 in RPMI 1640, G361 and SKMel28 in MEM, HMV-II in Ham's F12, and MMAc in DMEM. MC9, a mast cell line, was cultured in RPMI 1640 supplemented with 5% FCS, 50 μM 2-mercaptoethanol, and 6 ng/ml mouse recombinant IL-3. Cells were transfected by the calcium phosphate method with Cell Phect (Amersham) or by the lipofection method with FuGENE 6 (Roche). For retrovirus-mediated gene expression, NIH3T3 cells were infected with the retroviruses produced by PLAT-E as reported (Sasaki *et al.*, 2003). B16, B16F10, G361, and SKMel 28 cell lines were kindly provided by Dr Yonemitsu (Kyushu University, Japan).

Library screening

Retroviruses containing the human HeLa retroviral cDNA library (CLONTECH, Palo Alto, CA, USA) were produced from PLAT-E and 1×10^6 STAT3C-3T3 cells were infected with 10 ml of the retroviral supernatant containing 10 mg/ml polybrene. After 48 h of virus transduction, STAT3C-3T3 cells were seeded in soft-agar medium. Within 3 weeks, two colonies were picked up and expanded, and genomic DNA was isolated. Integrated cDNAs were recovered by PCR using a pair of primers (FWD, 5'-AGCCCTCACTCCTTCTCTAG, and REV, 5'-ATGGCGTTACTTAAGCTAGCTTGC-CAAACCTAC) and sequenced.

Colony formation in soft-agar

The MITF-infected 3T3 and STAT3C-3T3 cells were seeded into 35-mm dishes in suspensions of 0.36% Agar noble (Difco) in DMEM supplemented with 10% CS on top of a bed of 0.72% Agar noble in the same complete medium. The MITF-infected STAT3C-3T3 cells were inoculated with a retrovirus of dominant-negative AP-1 or an empty vector (Ui *et al.*, 2000), selected with puromycin, and plated into soft-agar medium. The cultures were incubated for 21 days and then the colonies were counted and photographed.

Construction of MITF

The cDNAs of wt-, ΔN-, and mi-MITF were subcloned into a bicistronic retrovirus vector pMX-IRES-EGFP (Nosaka *et al.*, 1999) or a pcDNA3 expression vector.

Retrovirus of dominant-negative AP-1

The control virus (pBabe-IRESpuro) and the SupJunD-1 virus (pBabe-SupJunD-1-IRESpuro) as a dominant-negative AP-1 were generated as described (Ui *et al.*, 2000). After infection, STAT3C-3T3 cells were cultured with 2 mg/ml puromycin.

High-density oligonucleotide microarray analysis

RNA was extracted by standard methods. Cells were lysed directly in their Petri dishes in TRIzol reagent (Invitrogen, Carlsbad, CA, USA) and total RNA was isolated according to

the manufacturer's instructions. cRNA preparation and microarray hybridization were carried out according to the supplier's instructions (Affymetrix, Santa Clara, CA, USA), using Genechip HG-U95Av2. Scanned output files were analysed by the probe level analysis package, Microarray Suite MAS 5.0 (Affymetrix, Santa Clara, CA, USA). The signal for each of these genes was determined from the 'probe set' in use for this gene and by the probe level analysis method provided by Affymetrix software.

Northern Blotting analysis and RT–PCR

Total RNA (10 μg) extracted from cells using TRIzol was evaluated by Northern blotting analysis with digoxigenin-labeled antisense RNA of c-*fos* and G3PDH labeled with the DIG RNA Labeling Kit (Roche). To determine the microarray data, 1 μg of total RNA was reverse-transcribed with the Reverse Transcribed Kit (Roche) and RT–PCR was performed with primers as follows: mouse MITF, 5′-GGAACAGCAAC-GAGCTAAGG and 5′-TGATGATCCGATTCACCAGA; human MITF, 5′-AGAACAGCAACGCGCAAAAGAAC and TGATGATCCGATTCACCAAATCTG; mouse GTP cyclohydrorase, 5′-GGCTGCTTACTCGTCCATTC and AG GTGATGCTCACACATGGA; mouse JE, AGGTCCCTGT CATGCTTCTG and TCTGGACCCATTCCTTCTTG; mouse PMEL17 CAGGGGTCTAACTGCTGGAG and TT CGGAGGTTTAGGACCAGA; mouse MRP8, GGAAAT CACCATGCCCTCTA and TGGCTGTCTTTGTGAGAT GC; mouse MARC, TCTGTGCCTGCTGCTCATAG and CTTTGGAGTTGGGGTTTTCA; and mouse MCPL, GCA CTTCTCTTGCCTTCTGG and TGTGCAGCAGTCATCA CAAA.

Western blotting analysis

Cells were lysed in a lysis buffer (50 mM Tris-HCl pH 7.4, 150 mM NaCl, 0.5% or 1% NP-40, 1 mM EDTA, 1 mM vanadate, 50 mM NaF, 1 mM DTT, 0.01 mM APMSF) and centrifuged at 12 000*g* for 10 min. The supernatants were resolved on SDS–PAGE of 10% gels, blotted, and immunostained with an anti-phospho STAT3 (Tyr705) polyclonal antibody (Cell Signaling Technology) and an anti-STAT3 polyclonal antibody (Santa Cruz Biotechnology).

Luciferase assay

An APRE-luciferase reporter gene for STAT3 activity and a reporter gene construct containing MITF-responsive mMCP-6 (mouse mast cell protease) luciferase have been described previously (Morii *et al.*, 1996; Yasukawa *et al.*, 1999). A c-*fos* promoter–reporter gene consisting of the c-*fos* promoter region containing SIE, SRE, and several potential MITF-binding motifs (Tsujimura *et al.*, 1996) is also described (Shibuya *et al.*, 1994; Kawahara *et al.*, 1995; Kim *et al.*, 1998). Luciferase assays were carried out using the dual-luciferase reporter system (Promega). The expression plasmid of STAT3-C in pRcCMV was kindly provided by Dr JE Darnell Jr (Bromberg *et al.*, 1999).

Nuclear extract preparation and oligonucleotide-binding assay

293T cells (1.5×10^7) were transfected with Myc-ΔN-MITF and STAT3C were stimulate with LIF for 6 h. Cells were collected and resuspended in 0.4 ml of buffer A (10 mM HEPES-KOH (pH 7.8), 10 mM KCl, 0.1 mM EDTA, 0.4% NP-40, 1 mM DTT, 0.5 mM APMSF, 2 μg/ml leupeptin, and 1 mM Na_3VO_4). After a brief vortexing and centrifugation, the supernatant was discarded and the nuclei-containing pellet was resuspended in 0.05 ml of buffer C (50 mM HEPES-KOH (pH 7.8), 420 mM NaCl, 5 mM $MgCl_2$, 0.1 mM EDTA, 2% glycerol, 1 mM DTT, 0.5 mM APMSF, 2 μg/ml leupeptin, and 1 mM Na_3VO_4) at 4°C for 30 min. The suspension was pelleted by centrifugation and the supernatants were collected and stored at −80°C until use. Oligonucleotide-conjugated beads were prepared using the DNA-binding protein purification kit (Roche) according to the manufacturer's protocol. In brief, the sense and antisense oligonucleotide of the human c-*fos* promoter sequence, including the SIE and SRE regions (5′-C AGTTCCCGTCAATCCCTCCCCCCTTACACAGGATGTC CATATTAGGACATCTGC-3′) were annealed, and they were ligated with the washed streptavidin magnetic particles for 30 min at 25°C. After ligation was carried out, the particles were washed using a magnetic separator and mixed with 100 μg of the nuclear extract for 30 min at 25°C. Then, the particles were washed and the DNA-binding proteins were eluted. The elutates were pelleted with trichloroacetic acid solution, and analysed by immunoblotting with anti-STAT3 and anti-Myc antibodies.

ChIP assay

For ChIP assay, 243T cells (5×10^6) were fixed with 1% formaldehyde for 10 min at 37°C, washed with PBS, and lysed in ChIP lysis buffer (Upstate Biotechnology, Lake Placid, NY, USA). DNA was sonicated by pulsing five times. Anti-acetylated histone H4 (Upstate), anti-STAT3 (Sigma), or anti-MITF monoclonal antibody (Oncogene), and anti-MITF polyclonal antibody (Santa Cruz Biotechnology) was added (5 μg–20 μg per immunoprecipitation) and incubated overnight. Protein A–agarose beads (Upstate Biotechnology) were added for 1 h and then washed once each with a low-salt buffer, high-salt buffer, and LiCl buffer. They were then washed twice with a TE buffer. The beads were eluted with 0.1 M NaHCO3 and 1% SDS, and crosslinks were reversed at 65°C. DNA was ethanol precipitated in the presence of 20 μg glycogen. PCR was carried out using primers specific to the promoter region of mouse c-*fos* (FWD, 5′-TCTGCCTTTCCCGCCTCCCC, and REV, 5′-GGCCGTGGAAACCTGCTGAC) for NIH3T3, and human c-fos (FWD, 5′-CCCGACCTCGGGAACAAGGG, and REV, 5′-ATGAGGGGTTTCGGGGATGG) for HMV-II, or (FWD, 5′-TCTCATTCTGCGCCGTTCCC, and REV, 5′-GGCCGTGGAAACCTGCTGAC) for G361.

Acknowledgements
We thank Dr T Yoshida (Kurume University) for STAT3C-3T3, Dr Yonemitsu (Kyushu University) for melanoma cell lines, H Meguro for oligonucleotide microarray analysis, Y Kawabata for technical assistance, and N Arifuku for manuscript preparation. This work was supported by special grants-in-aid from the Ministry of Education, Science, Technology, Sports, and Culture of Japan, the Japan Health Science Foundation, the Human Frontier Science Program, the Japan Research Foundation for Clinical Pharmacology, Haraguchi Memorial foundation, and the Uehara Memorial Foundation. AJ is supported by the fellowship from Japan Society for Promotion of Science.

References

Bowman T, Garcia R, Turkson J and Jove R. (2000). *Oncogene*, **19**, 2474–2488.

Bromberg J and Darnell Jr JE. (2000). *Oncogene*, **19**, 2468–2473.

Bromberg JF, Wrzeszczynska MH, Devgan G, Zhao Y, Pestell RG, Albanese C and Darnell Jr JE. (1999). *Cell*, **98**, 295–303.

Burd PR, Rogers HW, Gordon JR, Martin CA, Jayaraman S, Wilson SD, Dvorak AM, Galli SJ and Dorf ME. (1989). *J. Exp. Med.*, **170**, 245–257.

Carreira S, Liu B and Goding CR. (2000). *J. Biol. Chem.*, **275**, 21920–21927.

Darnell Jr JE. (1997). *Science*, **277**, 1630–1635.

Hatakeyama M, Kawahara A, Mori H, Shibuya H and Taniguchi T. (1992). *Proc. Natl. Acad. Sci. USA*, **89**, 2022–2026.

Hemesath TJ, Price ER, Takemoto C, Badalian T and Fisher DE. (1998). *Nature*, **391**, 298–301.

Kamaraju AK, Bertolotto C, Chebath J and Revel M. (2002). *J. Biol. Chem.*, **277**, 15132–15141.

Kawahara A, Minami Y, Miyazaki T, Ihle JN and Taniguchi T. (1995). *Proc. Natl. Acad. Sci. USA*, **92**, 8724–8728.

Kim DW, Cheriyath V, Roy AL and Cochran BH. (1998). *Mol. Cell. Biol.*, **18**, 3310–3320.

Kim DS, Hwang ES, Lee JE, Kim SY, Kwon SB and Park KC. (2003). *J. Cell Sci.*, **116**, 1699–1706.

Kitamura Y, Morii E, Jippo T and Ito A. (2002). *Mol. Immunol.*, **38**, 1173.

Kitamura T, Onishi M, Kinoshita S, Shibuya A, Miyajima A and Nolan GP. (1995). *Proc. Natl. Acad. Sci. USA*, **92**, 9146–9150.

Kobayashi T, Urabe K, Orlow SJ, Higashi K, Imokawa G, Kwon BS, Potterf B and Hearing VJ. (1994). *J. Biol. Chem.*, **269**, 29198–29205.

Kulmburg PA, Huber NE, Scheer BJ, Wrann M and Baumruker T. (1992). *J. Exp. Med.*, **176**, 1773–1778.

Levy C, Nechushtan H and Razin E. (2002). *J. Biol. Chem.*, **277**, 1962–1966.

Lufei C, Ma J, Huang G, Zhang T, Novotny-Diermayr V, Ong CT and Cao X. (2003). *EMBO J.*, **22**, 1325–1335.

Mansky KC, Marfatia K, Purdom GH, Luchin A, Hume DA and Ostrowski MC. (2002). *J. Leukocyte Biol.*, **71**, 295–303.

Matsui T, Kinoshita T, Hirano T, Yokota T and Miyajima A. (2002). *J. Biol. Chem.*, **277**, 36167–36173.

McGill GG, Horstmann M, Widlund HR, Du J, Motyckova G, Nishimura EK, Lin YL, Ramaswamy S, Avery W, Ding HF, Jordan SA, Jackson IJ, Korsmeyer SJ, Golub TR and Fisher DE. (2002). *Cell*, **109**, 707–718.

Morii E, Tsujimura T, Jippo T, Hashimoto K, Takebayashi K, Tsujino K, Nomura S, Yamamoto M and Kitamura Y. (1996). *Blood*, **88**, 2488–2494.

Morita S, Kojima T and Kitamura T. (2000). *Gene Therapy*, **7**, 1063–1066.

Nakayama K, Kim KW and Miyajima A. (2002). *EMBO J.*, **21**, 6174–6184.

Nosaka T, Kawashima T, Misawa K, Ikuta K, Mui AL and Kitamura T. (1999). *EMBO J.*, **18**, 4754–4765.

Nyormoi O and Bar-Eli M. (2003). *Clin. Exp. Metastasis*, **20**, 251–263.

Ogihara H, Morii E, Kim DK, Oboki K and Kitamura Y. (2001). *Blood*, **97**, 645–651.

Ong EK, Griffith IJ, Knox RB and Singh MB. (1993). *Gene*, **134**, 235–240.

Sasaki A, Inagaki-Ohara K, Yoshida T, Yamanaka A, Sasaki M, Yasukawa H, Koromilas AE and Yoshimura A. (2003). *J. Biol. Chem.*, **278**, 2432–2436.

Sato M, Morii E, Takebayashi-Suzuki K, Yasui N, Ochi T, Kitamura Y and Nomura S. (1999). *Biochem. Biophys. Res. Commun.*, **254**, 384–387.

Shibahara S, Takeda K, Yasumoto K, Udono T, Watanabe K, Saito H and Takahashi K. (2001). *J. Invest. Dermatol. Symp. Proc.*, **6**, 99–104.

Shibuya H, Kohu K, Yamada K, Barsoumian EL, Perlmutter RM and Taniguchi T. (1994). *Mol. Cell. Biol.*, **14**, 5812–5819.

Stark GR, Kerr IM, Williams BR, Silverman RH and Schreiber RD. (1998). *Annu. Rev. Biochem.*, **67**, 227–264.

Tachibana M. (1997). *Pigment Cell Res.*, **10**, 25–33.

Tsujimura T, Morii E, Nozaki M, Hashimoto K, Moriyama Y, Takebayashi K, Kondo T, Kanakura Y and Kitamura Y. (1996). *Blood*, **88**, 1225–1233.

Turkson J, Bowman T, Garcia R, Caldenhoven E, De Groot RP and Jove R. (1998). *Mol. Cell. Biol.*, **18**, 2545–2552.

Udono T, Yasumoto K, Takeda K, Amae S, Watanabe K, Saito H, Fuse N, Tachibana M, Takahashi K, Tamai M and Shibahara S. (2000). *Biochim. Biophys. Acta*, **1491**, 205–219.

Ui M, Mizutani T, Takada M, Arai T, Ito T, Murakami M, Koike C, Watanabe T, Yoshimatsu K and Iba H. (2000). *Biochem. Biophys. Res. Commun.*, **278**, 97–105.

Vachtenheim J, Novotna H and Ghanem G. (2001). *J. Invest. Dermatol.*, **117**, 1505–1511.

Yasukawa H, Misawa H, Sakamoto H, Masuhara M, Sasaki A, Wakioka T, Ohtsuka S, Imaizumi T, Matsuda T, Ihle JN and Yoshimura A. (1999). *EMBO J.*, **18**, 1309–1320.

Yoshida T, Hanada T, Tokuhisa T, Kosai K, Sata M, Kohara M and Yoshimura A. (2002). *J. Exp. Med.*, **196**, 641–653.

Yu CL, Meyer DJ, Campbell GS, Larner AC, Carter-Su C, Schwartz J and Jove R. (1995). *Science*, **269**, 81–83.

Zanocco-Marani T, Bateman A, Romano G, Valentinis B, He ZH and Baserga R. (1999). *Cancer Res.*, **59**, 5331–5340.